Electronic Supplementary Information

Experimental Section

Materials: Carbon cloth (CC) was bought from Hongshan District, Wuhan Instrument Surgical Instruments business, and treated in nitric acid (HNO_3) to serve as substrate for active materials. 50% manganese nitrate ($Mn(NO_3)_2$) solution and Cobaltous nitrate ($Co(NO_3)_2 \cdot 6H_2O$) was purchased from Aladdin Ltd. in Shanghai. Ammonium (NH_4F) and urea was provided by Beijing Chemical Works. HNO_3 and ethanol were purchased from Tianjin Chemical Corporation. $K_2B_4O_7 \cdot 4H_2O$ was purchased by Chengdu Kelon Chemical Reagent Factory. Pt/C (10 wt% Pt) was purchased from Alfa Aesar (China) Chemicals Co. Ltd. $RuCl_3 \cdot 3H_2O$ and Nafion (5 wt %) were bought from Sigma-Aldrich Chemical Reagent Co., Ltd. All chemical regents were used as received without further purification. Deionized water was made by the Millipore system and used in all experimental process.

Preparation of spinel $MnCo_2O_4$ nanowires array on carbon cloth ($MnCo_2O_4$/CC) and Mn-Co-borate nanowires array on carbon cloth (Mn-Co-Bi/CC): Typically, CC was first treated with concentrated HNO_3, ethanol and deionized water by sonication to achieve a clean surface before use. Then CC was put into deionized water (70 ml) containing $Mn(NO_3)_2$ (2 mmol), $Co(NO_3)_2 \cdot 6H_2O$ (4 mmol), urea (24 mmol) and NH_4F (10 mmol). After vigorous stirring for several minutes, the aqueous solution and CC were transferred to a 100 ml Teflon-lined stainless-steel autoclave. It was heated at 120 °C for 5 h to achieve the precursor. The resulting precursor was washed with deionized water for several times and further annealed at 300 °C in air to convert into $MnCo_2O_4$/CC. To realize the transformation of $MnCo_2O_4$/CC to Mn-Co-Bi/CC, $MnCo_2O_4$/CC was used as the working electrode in a three-electrode setup with the current density of 10 mA cm^{-2} in 0.5 M K-Bi (pH 9.2). After 2.5 h operating, the potential reaches a lowest value, indicating the successful synthesis of Mn-Co-Bi/CC.

Synthesis of RuO_2: RuO_2 was prepared in accordance with previous report.[1] Firstly, 2.61 g $RuCl_3 \cdot 3H_2O$ was dispersed in 100 mL distilled water and stirred for 10 minutes at 100 °C. Then 1.0 ml NaOH (1.0 M) was added into the above solution. And the mixture was under 100 °C for another 45 minutes. After cool to room temperature, the mixture was centrifuged to collect the precipitation, further dried at 80 °C for 12 h. The dried precipitation was annealed at 300 °C in Ar atomosphere to achieve RuO_2.

Characterizations: X-ray diffraction (XRD) measurements were performed using a RigakuD/MAX 2550 diffractometer with Cu Kα radiation (λ=1.5418 Å). Scanning electron microscopy (SEM) measurements were performed on a HITCHI S-4800 scanning electron microscope at an accelerating voltage of 25 kV. Transmission electron microscopy (TEM) measurements were made on a Zeiss Libra 200FE transmission electron microscope operated at 200 kV. X-ray photoelectron spectrometer (XPS) measurements were performed on an ESCALABMK II X-ray photoelectron spectrometer using Mg as the exciting source.

Electrochemical measurements: Electrochemical measurements were performed with a CHI 660E electrochemical analyzer (CH Instruments, Inc., Shanghai). In a typical three-electrode system, the $MnCo_2O_4$/CC or Mn-Co-Bi/CC was used as the working electrode, a graphite rod as the counter electrode and SCE as the reference electrode. The potentials reported in this work were converted to the RHE with the following equation: E (RHE) = E (SCE) + (0.24 + 0.0591 pH) V. Linear sweep voltammetry test was performed at a scan rate of 5 mV s^{-1} at room temperature (~25 °C). To calculate turnover frequency, cyclic voltammetry (CV) tests of $MnCo_2O_4$/CC and Mn-Co-Bi/CC were conducted with scanning rates of 5, 10, 15, 20, 25 mV s^{-1}, respectively.

TOF calculation: TO calculate TOF, the surface concentration of active sites related to the redox Mn and Co species was first obtained. According to the electrochemical CV curves (Fig. 3a and Fig. 3c), the oxidation peak current of redox species presents linear change on scan rates (Fig. 3b and Fig. 3d). The slope of the line can be calculated using the following equation:

$$slope = \frac{n^2 F^2 A \tau_0}{4RT}$$

Where n is the number of electrons transferred, F is Faraday's constant, A is the surface area of the electrode, τ_0 is the surface concentration of active sites (mol cm^{-2}), and R and T are the ideal gas constant and the absolute temperature, respectively. TOF values can be finally calculated based on the formula:

$$TOF = \frac{JA}{4FM}$$

J is the current density at certain overpotential, A is the area of the electrode, 4 indicates

the mole of electrons consumed for evolving one mole of O_2 from water, F is Faraday's constant and m is the number of moles for active sites.

Determination of Faradaic efficiency (FE): FE was calculated by comparing the amount of experimentally quantified gas with theoretically calculated gas. The experimentally evolved gas was confirmed by gas chromatography (GC) analysis and measured quantitatively by monitoring the pressure change via a calibrated pressure sensor in the anode compartment of an H-type electrolytic cell. The number of theoretically evolved gas was calculated by presuming that all charges through the $4e^-$ oxidation for oxygen production and $2e^-$ reduction for hydrogen production.

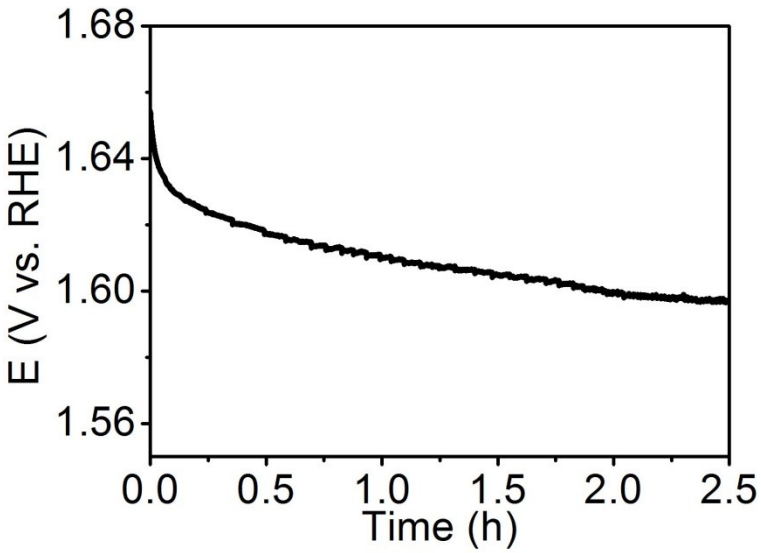

Fig. S1. Chronopotentiometric curve for oxidative polarization.

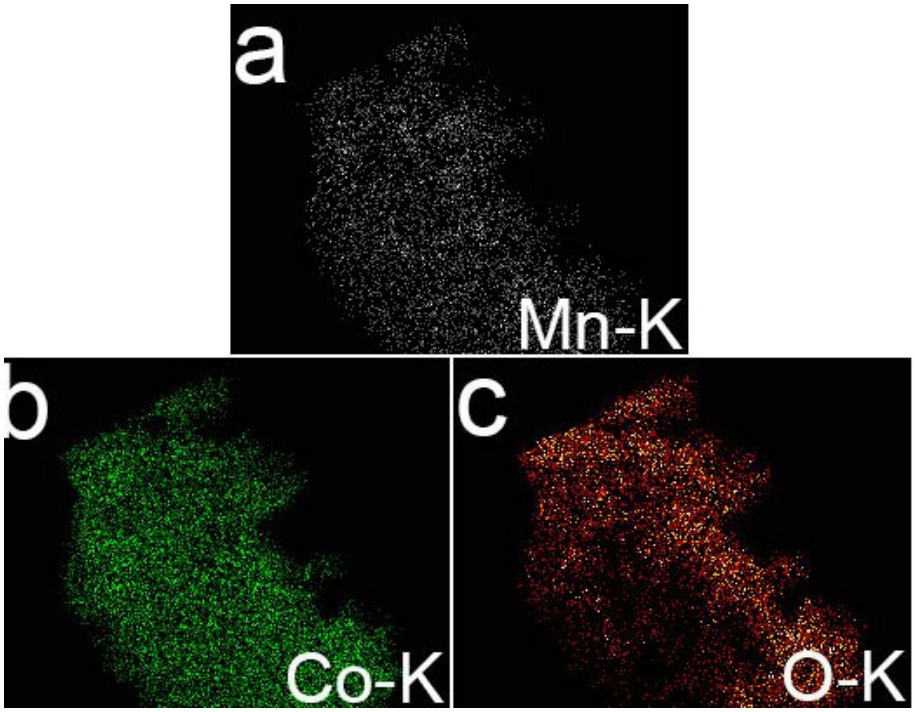

Fig. S2. The EDX elemental mapping of (a) Mn, (b) Co and (c) O for $MnCo_2O_4$/CC.

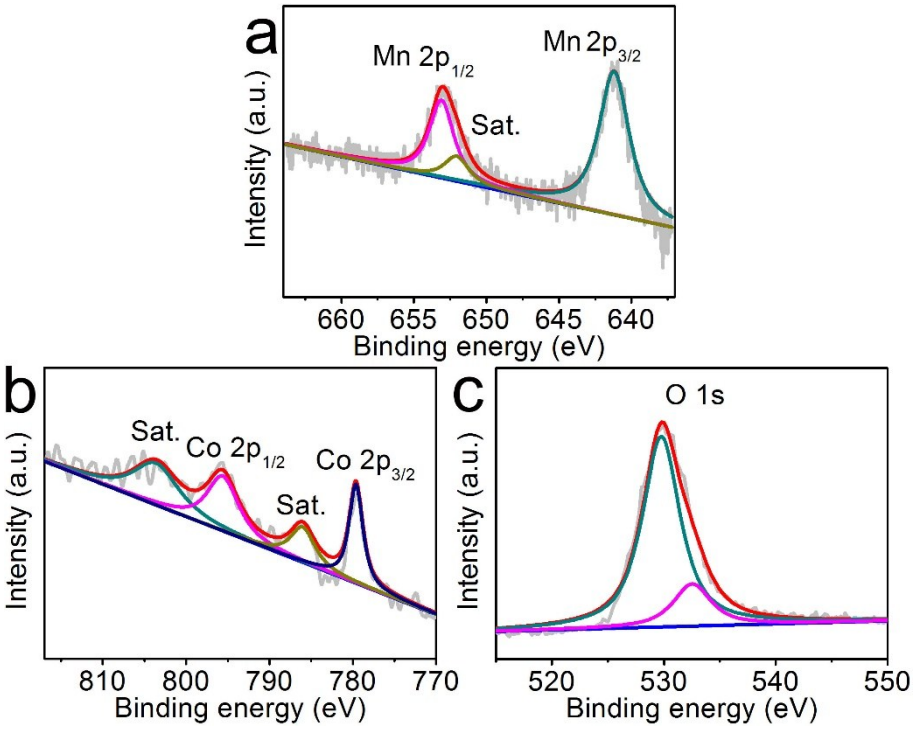

Fig. S3. XPS spectra of $MnCo_2O_4$/CC in the (a) Mn 2p, (b) Co 2p and (c) O 1s region.

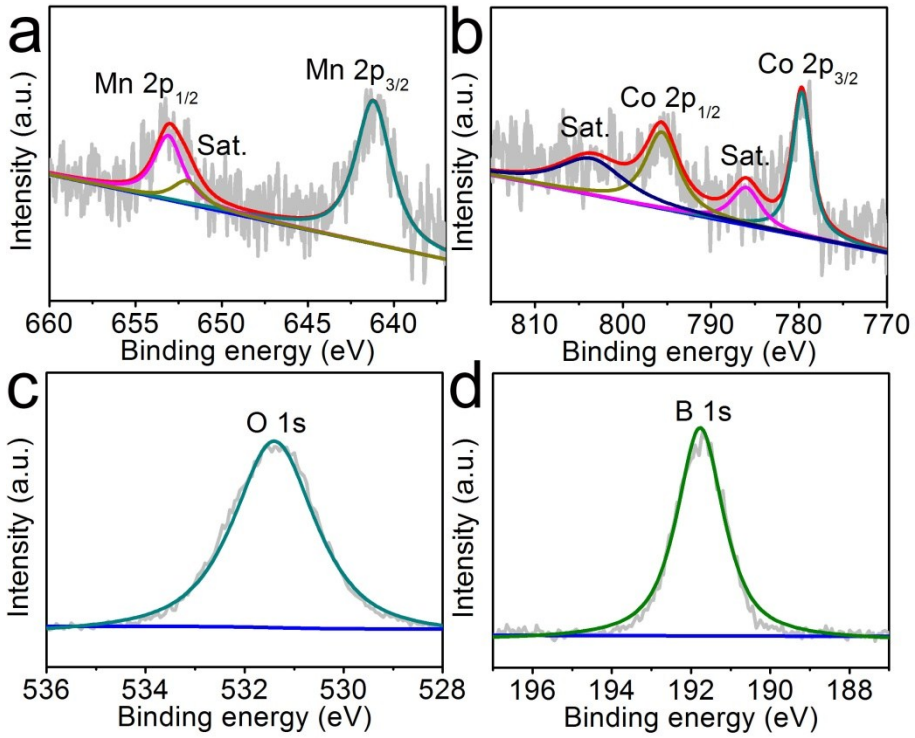

Fig. S4. XPS spectra of Mn-Co-Bi/CC in the (a) Mn 2p, (b) Co 2p (c) O 1s and (d) B 1s region.

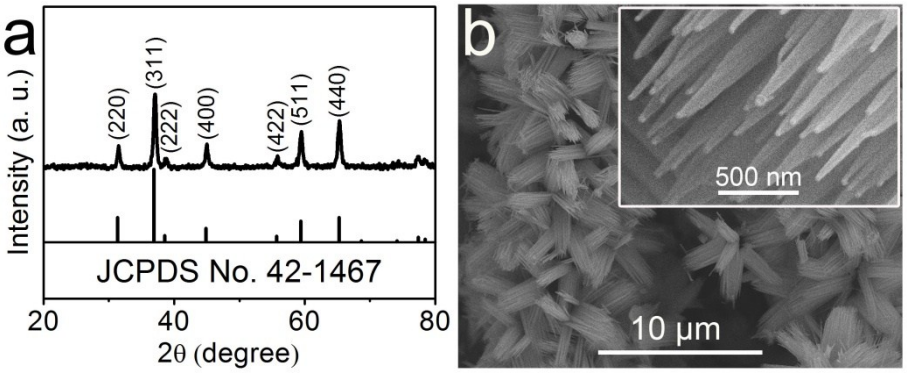

Fig. S5. (a) XRD patterns of Co_3O_4/CC. (b) SEM image for Co_3O_4/CC.

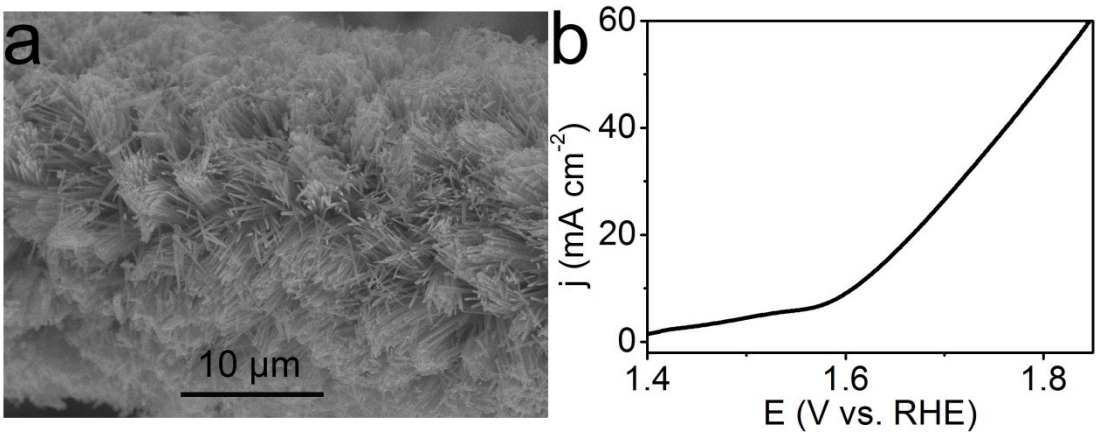

Fig. S6. (a) SEM image for Co_3O_4-derived nanowires array catalyst. (b) Polarization curve for such catalyst with a scan rate of 5 mV s^{-1} for OER in 0.5 M K-Bi.

Table S1. Comparison of OER performance for Mn-Co-Bi/CC with other non-noble-metal electrocatalysts in neutral or near-neutral media..

Catalyst	j (mA cm^{-2})	η (mV)	Electrolyte	Refs.
Mn-Co-Bi	10	418	0.1 M K-Bi	This work
	10	366	0.5 M K-Bi	
Ni-Bi/FTO	1	384	0.5 M K-Bi	2
Ni-Bi/FTO	1	540	0.5 M K-Bi	3
NiO_x/MWCNT	0.5	330	0.1 M K-Bi	4
NiO_x-Bi	1	650	0.5 M K-Bi	5
NiO_x-Fe-Bi	5	552		
Co-Bi/FTO	1	390	1 M K-Bi	6
Co-W/FTO	1	420	0.05 M K-Bi	7
CuO/FTO	0.1	430	0.1 M K-Bi	8
Cu-TPA/FTO	0.18	320	0.1 M K-Bi	9
Ni-Bi/CC	10	470	0.1 M K-Bi	10
	10	390	0.5 M K-Bi	
Ni-Bi film/ITO	1	425	0.1 M Bi	11
Ni-Bi film/FTO	1	390	0.5 M K-Bi	12
Co-Pi/Ni foam	100	363	1 M K-Bi	2
NiO_x-en/FTO	1	510	0.6 M Na-Bi	6
Co_3O_4 nanorod	1	385	0.1 M K-Bi	6
MnO/FTO	5	530	0.3 M Na-Pi	13

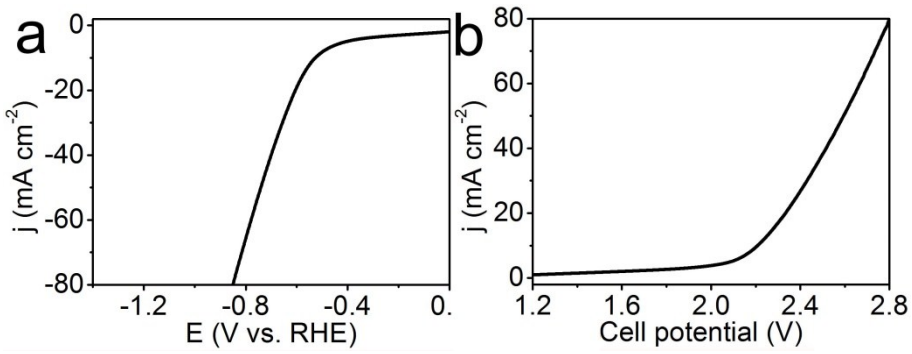

Fig. S7. (a) Polarization curve for Co_3O_4-derived nanoarray catalyst with a scan rate of 5 mV s^{-1} for HER in 0.5 M K-Bi. (b) Polarization curve of Co_3O_4-derived nanoarray catalyst couple for full water splitting with a scan rate of 5 mV s^{-1} in 0.5 M K-Bi.

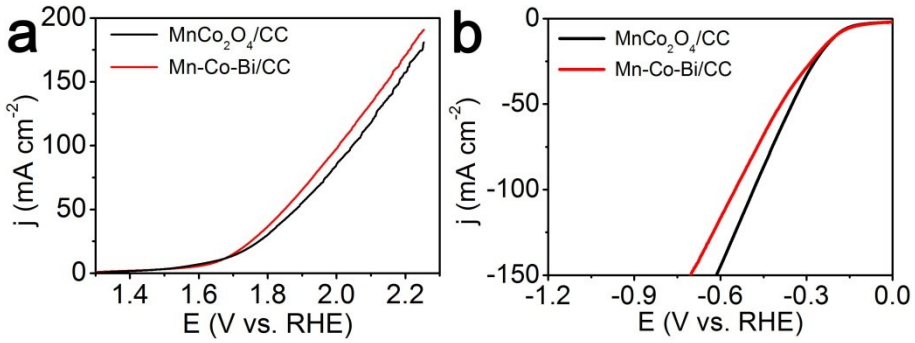

Fig. S8. (a) Polarization curves of $MnCo_2O_4$/CC and Mn-Co-Bi/CC for OER in 1.0 M PBS. (b) Polarization curves of $MnCo_2O_4$/CC and Mn-Co-Bi/CC for HER in 1.0 M PBS.

Table S2. Comparison of HER performance for $MnCo_2O_4$/CC with other non-noble-metal electrocatalysts in neutral or near-neutral media.

Catalyst	j (mA cm^{-2})	η (mV)	Electrolyte	Refs.
$MnCo_2O_4$/CC	10	293	0.5 M K-Bi	This work
	20	385		
Ni-Bi film/FTO	1.5	425	0.1 M Na-Bi	14
Cu-TPA/FTO	1	440	0.1 M K-Bi	9
Cu-EA/FTO	2	270	0.1 M K-Pi	15
H2-CoCat/FTO	2	385	0.5 M K-Pi	16
$CoO/CoSe_2$	10	337	0.5 M PBS	17
Co@nitrogen-rich carbon nanotubes	10	540	0.1 M PBS	18
FeS	0.7	450	0.1 M PBS	19
MoP/CF	1	300	1.0 M PBS	20
Cu/Cu_2O	8	310	0.5 M KPi	21
$MoS_{2.7}$@NPG	0.48	200	0.2 M PBS	22
WO_3 NAs/CC	10	302	1.0 M PBS	23
CoP/CC	10	106	1.0 M PBS	24
Co-Mo-S film	1.04	200	PBS	25
Mo_2C	1	200	PBS	26
Cu(0) based film	10	333	0.5 M PBS	27

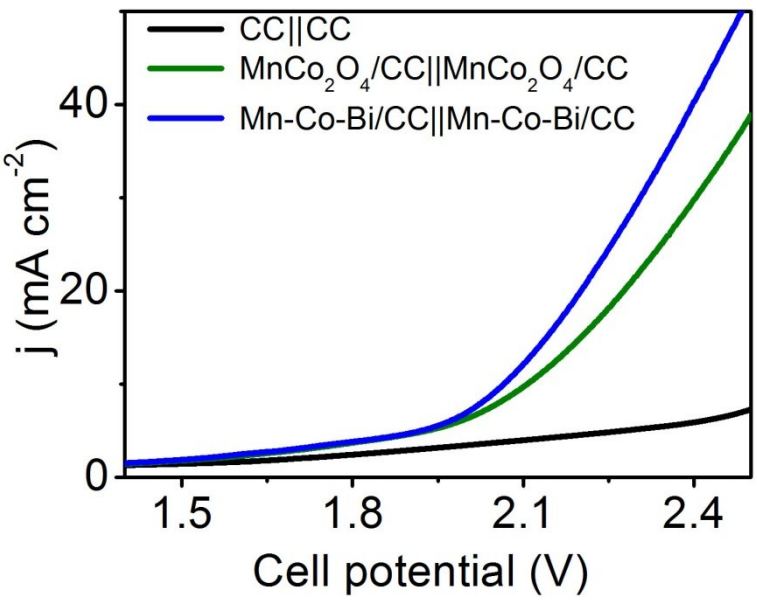

Fig. S9. Polarization curves of CC||CC, $MnCo_2O_4$/CC||$MnCo_2O_4$/CC and Mn-Co-Bi/CC||Mn-Co-Bi/CC for full water splitting with a scan rate of 5 mV s^{-1}.

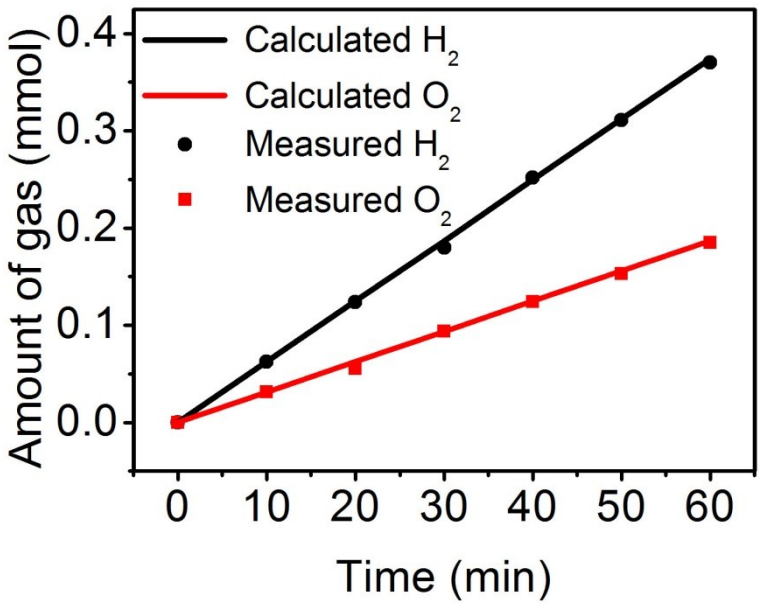

Fig. S10. The amount of gas theoretically calculated and experimentally measured vs. time for overall water splitting of $MnCo_2O_4$/CC||Mn-Co-Bi/CC.

References

1 J. C. Cruz, V. Baglio, S. Siracusano, V. Antonucci, A. S. Aricò, R. Ornelas, L. Ortiz-Frade, G. Osorio-Monreal, S. M. Durón-Torres and L. G. Arriaga, *Int. J. Electrochem. Sci.*, 2011, **7**, 6607-6619.

2 D. K. Bediako, Y. Surendranath and D. G. Nocera, *J. Am. Chem. Soc.,* 2013, **135**, 3662-3674.

3 I. M. Roger and D. Symes, *J. Am. Chem. Soc.,* 2015, **137**, 13980-13988.

4 X. Yu, T. Hua, X. Liu, Z. Yan, P. Xu and P. Du, *ACS Appl. Mater. Interfaces,* 2014, **6**, 15395-15402.

5 A. Singh, S. L. Y. Chang, R. K. Hocking, U. Bach and L. Spiccia, *Energy Environ. Sci.,* 2013, **6**, 579-586.

6 A. J. Esswein, Y. Surendranath, S. Y. Reece and D. G. Nocera, *Energy Environ. Sci.,* 2011, **4**, 499-504.

7 B. Zhang, X. Wu, F. Li, F. Yu, Y. Wang and L. Sun, *Chem. Asian J.,* 2015, **10**, 2228-2233.

8 X. Liu, S. Cui, Z. Sun and P. Du, *Electrochim. Acta,* 2015, **160**, 202-208.

9 X. Liu, H. Zheng, Z. Sun, A. Han and P. Du, *ACS Catal.,* 2015, **5**, 1530-1538.

10 X. Ji, L. Cui, D. Liu, S. Hao, J. Liu, F. Qu, Y. Ma, G. Du, A. M. Asiri and X. Sun, Chem. Commun., 2017, 53, 3070-3073.

11 M. Dincă, Y. Surendranath and D. G. Nocera, *Proc. Natl. Acad. Sci. U. S. A*., 2010, 107, 10337-10341.

12 D. K. Bediako, Y. Surendranath and D. G. Nocera, *J. Am. Chem. Soc.*, 2013, **135**, 3662-3674.

13 K. Jin, A. Chu, J. Park, D. Jeong, S. E. Jerng, U. Sim, H. Jeong, C. W. Lee, Y. Park, K. D. Yang, G. K. Pradhan, D. Kim, N. Sung, S. H. Kim and K. T. Nam, *Sci. Rep*., **2015**, *5*, 10279.

14 C. He, X. Wu and Z. He, *J. Phys. Chem. C,* 2014, **118**, 4578-4584.

15 X. Liu, S. Cui, Z. Sun and P. Du, *Chem. Commun.,* 2015, **51**, 12954-12957.

16 S. Cobo, J. Heidkamp, P. Jacques, J. Fize, V. Fourmond, L. Guetaz, B. Jousselme, V. Ivanova, H. Dau, S. Palacin, M. Fontecave and V. Artero, *Nat. Mater.,* 2012, **11**, 802-807.

17 K. Li, J. Zhang, R. Wu, Y. Yu and B. Zhang, *Adv. Sci.*, 2016, **3**, 1500426.

18 X. Zou, X. Huang, A. Goswami, R. Silva, B. R. Sathe, E. Mikmekovà and T. Asefa, *Angew. Chem, Int. Ed.*, 2014, **53**, 4372-4376.

19 C. D. Giovanni, W. Wang, S. Nowak, J. Greneche, H. Lecoq, L. Mouton, M. Giraud and C. Tard, *ACS Catal.,* 2014, **4**, 681-687.

20 W. Cui, Q. Liu, Z. Xing, A. M. Asiri, K. A. Alamry and X. Sun, *Appl. Catal. B-Environ.,* 2015, **164**,144-150.

21 J. Zhao, P. D. Tran, Y. Chen, J. S. C. Loo, J. Barber and Z. J. Xu, *ACS Catal.*, 2015, **5**, 4115-4120.

22 X. Ge, L. Chen, L. Zhang, Y. Wen, A. Hirata and M. Chen, *Adv. Mater.*, 2014, **26**, 3100-3104.

23 J. Shi, Z. Pu, Q. Liu, A. M. Asiri, J. Hu and X. Sun, *Electrochimica Acta,* 2015*,* **154***,* 345-351.

24 J. Tian, Q. Liu, A. M. Asiri and X. Sun, *J. Am. Chem. Soc.,* 2014, **136**, 7587-7590.

25 D. Merki, H. Vrubel, L. Rovelli, S Fierro and X. Hu, *Chem. Sci.,* 2012, **3**, 2515-2525.

26 H. Vrebel and X. Hu, *Angew. Chem., Int. Ed.,* 2012, **51**, 12703-12706.

27 J. Du, J. Wang, L. Ji, X. Xu and Z. Chen, *ACS Appl. Mater. Interfaces,* 2016, **8**, 30205-30211.